

Excitation of Thermoacoustic Instabilities by Interaction of Acoustics and Unstable Swirling Flow

Christian Oliver Paschereit*

ABB Corporate Research Ltd., 5405 Baden, Switzerland

Ephraim Gutmark†

Louisiana State University, Baton Rouge, Louisiana 70803-6413

and

Wolfgang Weisenstein‡

ABB Corporate Research Ltd., 5405 Baden, Switzerland

Unstable thermoacoustic modes were investigated and controlled in an experimental low-emission swirl stabilized combustor, in which the acoustic boundary conditions were modified to obtain combustion instability. The acoustic boundary conditions of the exhaust system could be adjusted from almost anechoic (reflection coefficient $|r| < 0.2$) to open-end reflection. Several axisymmetric and helical unstable modes were identified for fully premixed and diffusion-type combustion. These unstable modes were associated with flow instabilities related to the recirculation wake-like region on the combustor axis and shear-layer instabilities at the sudden expansion (dump plane). The combustion structure associated with the different unstable modes was visualized by phase-locked images of OH chemiluminescence. The axisymmetric mode showed large variation of the heat release during one cycle, whereas the helical modes showed variations in the radial location of maximal heat release. The axisymmetric mode was the dominant one during unstable combustion. It was obtained by forcing a longitudinal low-frequency acoustic resonance. Helical modes could only be obtained when the axisymmetric mode was suppressed by using a nonreflecting boundary condition. A closed-loop active control system was employed to suppress the thermoacoustic pressure oscillations and to reduce NO_x and CO emissions. Microphones were used to monitor the pressure oscillations during the combustion process and provide input to the control system. An acoustic actuation was used to modulate the airflow and thus affected the mixing process and the combustion. Upstream excitation modified the shear-layer structure and was shown to be superior to downstream excitation, which combined less effective shear-layer excitation with noise cancellation. Suppression levels of up to 5 dB in the pressure oscillations and a concomitant 24% reduction of NO_x emissions were obtained in premixed combustion using an acoustic power of less than 0.002% of the combustion power. The control of the diffusion flame was less effective, and NO_x emissions increased at the phase that was most effective in suppressing the pressure oscillations. The differences between the behavior of the control system in the two combustion modes was caused by different levels of interaction between the combustion process and the shear layer.

Introduction

LARGE-SCALE coherent structures play an important role in combustion and heat-release processes by controlling the mixing between fuel and air in diffusion-flame configurations and the mixing between the fresh fuel/air mixture and hot combustion products and fresh air in premixed combustors. The evolution of these structures in nonreacting flows was extensively studied in mixing layers,^{1,2} jets,^{3,4} and flows over backward-facing steps.⁵ However, studies of large structures in swirling flows are scarce. Unlike large-scale structures in nonswirling flows that are predominantly axisymmetric, swirl enhances azimuthal unstable modes. Interaction between large-scale structures that are related to flow instabilities, acoustic resonant modes in the combustion chamber, and the heat-release process was shown to cause undesired thermoacoustic instabilities in the combustor. The effect of swirl on the longitudinal and azimuthal instability modes and the way it modifies the combustion process leading to thermoacoustic instabilities requires further investigation.

Realizing the importance of large-scale structures as drivers of combustion instabilities, researchers developed passive and active methods to control this instability by modifying the vortical structures in the flow.⁶⁻⁸ Most of these control methods were applied to bluff-body-stabilized combustors and dump combustors in which the flow recirculation is used to stabilize the flame. Passive and active control strategies have been used to suppress thermoacoustic instabilities resulting from coupling between the heat and pressure oscillations in these combustors (Rayleigh criterion). Active control techniques used acoustic excitation of air and/or fuel modulations with phase-shifting strategies to decouple the pressure and heat-release cycles. Acoustic excitation was used either to modify the mixing patterns in the combustion chamber or to break the acoustic pressure feedback via antisound methodology. The former method proved to be more efficient because of the exponential amplification of the excitation signal by flow instabilities.⁹ The physical mechanism of the control system operation was different for premixed flames, in which mixing between hot combustion products and fresh air/fuel flow was affected, and diffusion flames where mixing of fuel and air was modified.¹⁰

Control strategies have also investigated improving fuel efficiency and reducing pollutants¹¹⁻¹³ and extending flammability limits.¹⁴

Although many papers describe control of nonswirling gaseous flames, a minimal amount of work was reported on control of swirling combustion. Swirl stabilization is used in combustion systems such as gas turbines, which also exhibit combustion instabilities.^{15,16} Rational modification of large-scale vortices is important to control swirl-induced instability and to increase combustion efficiency. However, flow control has been demonstrated primarily

Received 26 October 1998; revision received 12 July 1999; accepted for publication 18 November 1999. Copyright © 2000 by the American Institute of Aeronautics and Astronautics, Inc. All rights reserved.

*Group Leader; oliver.paschereit@chrcr.abb.ch.

†Voorhies Professor, Mechanical Engineering Department; currently Ohio Eminent Scholar and Professor, Aerospace Engineering and Engineering Mechanics Department, University of Cincinnati, Cincinnati, OH 45221; egutmark@uceng.uc.edu.

‡Research Engineer; wolfgang.weisenstein@chrcr.abb.ch.

for nonswirling flows, in which the large-scale instabilities are well understood, and the coherence of the vortices can be enhanced by flow excitation. Control of swirling flows requires the understanding of the vortical structure in this type of flow and the studying of the effect of forcing.

In the present work instability modes in an experimental low-emission swirl-stabilized combustor were investigated and acoustically controlled. The two operating modes that were studied included a partially premixed-diffusion flame and premixed combustion. The diffusion flame was tuned to unstable operation with two destabilized modes, axisymmetric and helical. The premixed instability modes were obtained by adjusting the acoustic boundary conditions. For changing the acoustic boundary condition orifices with different exit areas were used. The reflection coefficient was measured using a multimicrophone method.¹⁷ An axisymmetric mode flame instability mode was obtained by adjusting the combustor length and the acoustic boundary condition at the combustor exit to an acoustic reflection coefficient $|r| > 0.5$, which yielded a longitudinal plane wave acoustic mode. When the acoustic boundary condition was adjusted to almost anechoic conditions $|r| < 0.15$, a helical flame instability was observed. Pressure fluctuations were detected only for the axisymmetric modes, but heat-release fluctuations, which were measured by OH chemiluminescent emission, indicated dual-mode behavior. The effect of acoustic excitation on the unstable combustion was investigated using upstream and downstream located loudspeakers. A closed-loop active control system was employed to suppress combustion instabilities and to reduce emissions at various operating conditions. The effect of the control system on the unstable modes structure and combustor performance is reported. The choice of acoustic excitation for combustion control provides the opportunity to investigate the effect of airflow excitation and shear-flow modifications on the combustion dynamics. The more practical means of fuel modulations for combustion control are described elsewhere.¹⁸

Experimental Setup

Combustion Facility

The combustion facility is shown in Fig. 1. The atmospheric test rig consists of a plenum chamber upstream of the swirl-inducing burner nozzle and a combustion chamber downstream of the burner nozzle. The plenum chamber contains perforated plates to reduce the turbulence level of the flow. The circular combustion chamber consists of an air-cooled double-wall quartz glass to provide full visual access to the flame. The exhaust system is an air-cooled tube with the same cross section as the combustion chamber to avoid acoustic reflections at area discontinuities. The acoustic boundary conditions of the exhaust system could be adjusted from almost anechoic (reflection coefficient $|r| < 0.15$) to open-end reflection. An

experimental swirl-stabilized burner nozzle was used. Experiments were done in two operational modes: premixed combustion and partially premixed combustion, which was a quasi-diffusion flame. In the premixed mode natural gas was injected upstream of the swirling air to premix the fuel with the air. The flame was stabilized in a recirculation region near the burner nozzle outlet. During nonpremixed combustion, a pilot flame was used, and the fuel was injected into the recirculation region resulting in a quasi-diffusion flame. Controlled excitation of the burner nozzle flow was accomplished by a circumferential array of four loudspeakers equally spaced in polar angle. The four speakers provided the possibility to excite the flow with axisymmetric and higher modes depending on the relative phase of the driving signals. When operated at zero phase difference, they provided the acoustic energy necessary to achieve full control authority at the maximum heat-release level. One set of loudspeakers was placed at an axial distance of $x/D = 4.2$ upstream of the dump plane and the second set at $x/D = 9.6$ downstream of the dump plane. The nominal power of the 330-mm speakers was 120 W. For axisymmetric disturbances the loudspeakers were operated at zero phase difference. Forcing was possible upstream and downstream of the burner nozzle.

Measurement Techniques

Pressure fluctuations were measured using wall-mounted water-cooled $\frac{1}{4}$ -in. (6.35-mm) condenser microphones placed at an axial distance of $x/D = 2.5$. The holders consisted of a small orifice ($d = 1$ mm) open to the combustion chamber. The microphone diaphragm was placed in a small cavity and was heat radiation protected. The resonance frequency of the holder was larger than $f_{res} > 20$ kHz. Using condenser microphones rather than piezoelectric pressure probes gave the advantage of highly accurate data in phase and amplitude necessary for acoustic measurements. The frequency response of the microphones in probe holders were compared against standard B&K microphones and showed good agreement. A special test rig allowed for phase and amplitude calibration of the different microphone holders.

To measure acoustic quantities, as acoustic pressure and velocity, the same methods as in nonreacting systems can be used. The two-microphone method as described by Chung and Blaser¹⁹ has more practical relevance than the standing wave-tube method. It was extended to include the effect of mean flow.

To determine the acoustic characteristics of the burner nozzle/flame, the up- and downstream propagating waves f and g (Riemann invariants) have to be determined. The Riemann invariants are related to pressure and velocity by

$$p(\omega)/\rho c = f + g \quad (1)$$

$$u(\omega) = f - g \quad (2)$$

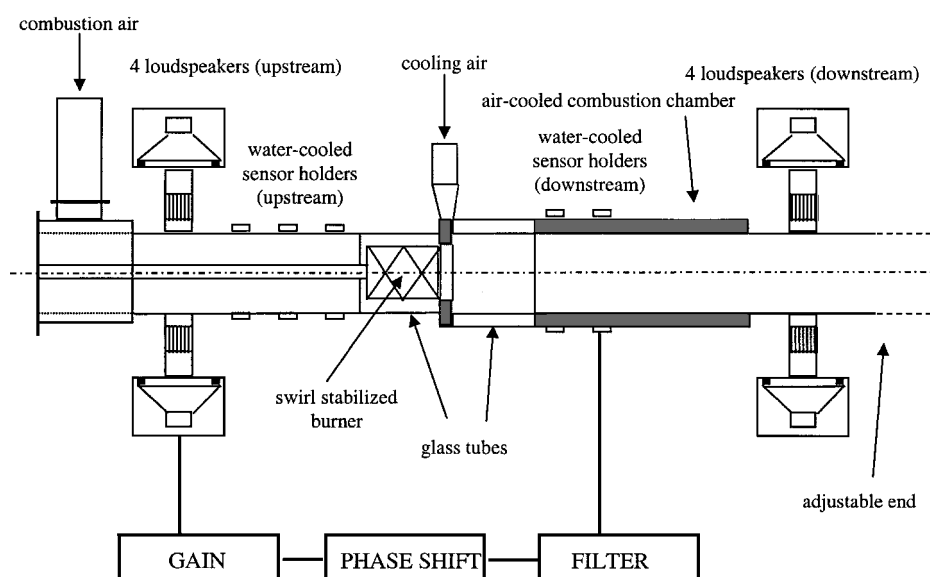


Fig. 1 Experimental arrangement of the combustor and schematic diagram of the control system.

At least two microphones are required for this type of measurement. Using two microphones at two different axial positions x_1 and x_2 in a tube, the Riemann invariants f and g at cross section x_1 are given by

$$\begin{bmatrix} f(x_1) \\ g(x_1) \end{bmatrix} = \frac{1}{\Phi^- - \Phi^+} \begin{pmatrix} 1 & 1 \\ \Phi^+ & \Phi^- \end{pmatrix} \begin{bmatrix} p(x_1) \\ p(x_2) \end{bmatrix} \quad (3)$$

where $\Phi^\pm = \exp[-ik_\pm(x_2 - x_1)]$ and $k_\pm = (\omega/c)/(M \pm 1)$. Once the Riemann invariants are known at location x_1 , they can be stepped into any location x_i , using the relations

$$f(x_i) = f(x_1)e^{-ik_+(x_i - x_1)}, \quad g(x_i) = g(x_1)e^{-ik_-(x_i - x_1)} \quad (4)$$

Acoustic properties such as impedance $Z = p/u$ or the acoustic reflection coefficient $r = g/f$ can then be calculated from the measured Riemann invariants.

In the present approach an extension of the two-microphone method, the multimicrophone method¹⁷ was used to improve the accuracy of the measured data. Using two pressure signals, it was possible to measure exactly the two quantities, i.e., the incident and the reflected wave components. By making more pressure measurements, the number of equations is larger than the number of unknowns, thus the problem is overdetermined. The calculated incident $f(x_i)$ and reflected $g(x_i)$ wave components were fitted to the measured quantities $p(x_i)$ by using the nonlinear Levenberg-Marquardt method to minimize the χ^2 quantity in the frequency domain:

$$\chi^2 = \sum_{i=0}^{N-1} \{ [f(x_i) + g(x_i)] - p(x_i) \}^2 \quad (5)$$

Time-varying heat release was recorded with two-filtered fiber optic probes to detect OH radiation. Several studies have shown that OH appears in superequilibrium concentrations in the flame front region.²⁰ Therefore, the OH emissions were used as a qualitative indicator to detect the heat release at the active combustion regions. The signal was bandpass filtered with a lower and higher cutoff wavelength of 290 and 390 nm. The circular field of view of the probes had a diameter of $d = 10$ mm at the flame position. The probe was coupled with a photomultiplier with a response time of 1 ns. The probe monitored the upper shear layer ($r/D = 0.5$) at an axial distance $x/D = 0.514$ downstream from the dump plane.

The operation conditions of the burner nozzle have been maintained by analyzing the exhaust gas composition using a physical gas analysis system. CO and CO₂ have been analyzed by using nondispersive infrared spectroscopy. The nitric oxides NO and NO₂, combined in NO_x, have been detected with a chemiluminescence analyzer. The detection of the remaining O₂ in the exhaust gas was made utilizing the paramagnetic properties of oxygen in the analyzing device. Carbon and oxygen balances were continuously computed, and agreement within 0.2% was assured.

Control and Structure Visualization Systems

A schematic diagram of the closed-loop control system is given in Fig. 1. The signals of the sensors (either microphone or OH emission probe) were amplified and bandpass filtered. The resulting signal was then used to trigger a signal generator to produce a phase-shifted signal at the instability frequency, which was fed back to drive the loudspeakers through an audio amplifier. Phase-locked pictures of the flame were obtained using an amplified (microchannel plate) charge-coupled device (CCD) camera with an exposure time of 20 μ s. The camera was triggered by using either the pressure or OH signals, which were bandpass filtered at the instability frequency and phase shifted. The images were filtered using a bandpass filter with a lower and higher cutoff wavelength of 290 and 390 nm, respectively. The phase-locked exposures were then averaged over 64 events.

Results and Discussion

Acoustic Boundary Conditions

The test rig instrumented with microphones allowed for high-accuracy acoustic measurements. Azimuthal and axisymmetric

combustion instabilities required different acoustic boundary conditions. The helical instabilities could only be obtained when no axisymmetric mode associated with a longitudinal acoustic mode was present in the combustor. This was achieved by tuning the acoustic boundary condition at the combustor exit to a small reflection coefficient r using an orifice. Here, the reflection coefficient $r = g/f$ is the ratio between the reflected wave component g and the incident wave component f . The reflection coefficient is thus a measure of the amount of the acoustic wave amplitude being reflected. Complete reflection will be achieved by a solid wall ($r = 1$) and by an open end ($r \approx -1$). To inhibit completely the feedback cycle in the combustion chamber by the reflected acoustic wave, the acoustic boundary condition at the end of the combustor must be tuned to be anechoic ($r = 0$). In this case no acoustic wave will be reflected by the tube exit. The results using an orifice to tune the acoustic boundary condition to a lower reflection coefficient are displayed in Fig. 2 and compared to the reflection coefficient of an open end following the theory of Levine and Schwinger.²¹ Displayed are the real and imaginary part of the reflection coefficient as well as its absolute value and phase. The absolute value of the reflection coefficient was reduced to about $r = 0.2$ – 0.3 in the region $100 < f < 300$ Hz, which is 20–30% of the open-end case. With combustion a pure tone excitation had to be used because of the high noise level of the combustion. Without combustion white noise excitation was used to measure the acoustic reflection coefficient. The results are displayed in Fig. 3 and show even smaller reflection down to $|r| = 0.1$. Axisymmetric combustion instabilities were then obtained by adjusting the acoustic boundary conditions close to open-end reflection, which allowed for a strong reflection of the incident waves, thus allowing a feedback cycle. The helical combustion instabilities could be forced to occur by using the orifice with a small reflection coefficient $r \approx 0.2$.

Upstream and Downstream Forcing

The testing facility was designed to enable the application of acoustic forcing from either upstream of the burner nozzle or from downstream of the combustion chamber (Fig. 1). To select the most efficient mode of operation, the effect of each one of the excitation modes on the flow structure and the resulting reaction rate was determined. The structure of the reacting vortices inside the combustor was assessed from axial and radial cross-spectral measurement between two OH chemiluminescence filtered fiber-optic probes. For the radial cross correlations one of the OH sensors was stationary in the upper shear layer at an axial distance of $x/D = 0.514$ from the dump plane, monitoring the shear-layer flow, whereas the other one was traversing the combustion zone radially at the same axial distance. It was moving radially starting from the stationary probe ($r/D = 0$) until it reached the opposite shear layer. The axial cross-correlation measurements were performed by positioning the upstream probe on the combustor's centerline or in the shear layer at a distance of $x/D = 0.514$, while the other probe was moved downstream, increasing the axial distance Δx between the probes. The measurements were compared for upstream and downstream forcing at two unstable Strouhal numbers $Sr = 1.16$ (helical instability) and 0.22 (axisymmetric instability). The Strouhal number Sr is a normalized frequency defined as $Sr = fD/\bar{U}$, where f is the instability frequency, D the burner nozzle diameter, and \bar{U} the burner nozzle mean exit velocity.

The coherence function, the amplitude of the radial and axial cross spectra, and the relative phase were measured at increased spacing between the two probes (Δr and Δx , respectively). The relative phase angles between the two OH signals are plotted as a function of $\Delta r/D$ in Fig. 4. The instabilities at $Sr = 1.16$ underwent a phase change of 180 deg corresponding to helical modes while the mode at $Sr = 0.22$ remained close to zero phase angle across the combustor, indicative of a quasi-axisymmetric mode. The differences between upstream and downstream forcing were not reflected in the radial phase variation. The two Strouhal numbers were related to different flow instabilities. When the flow instability frequencies matched the acoustic modes of the combustion chamber, they eventually grew to large-amplitude combustion instability. The effect of the upstream and downstream forcing on the amplitudes of both axial

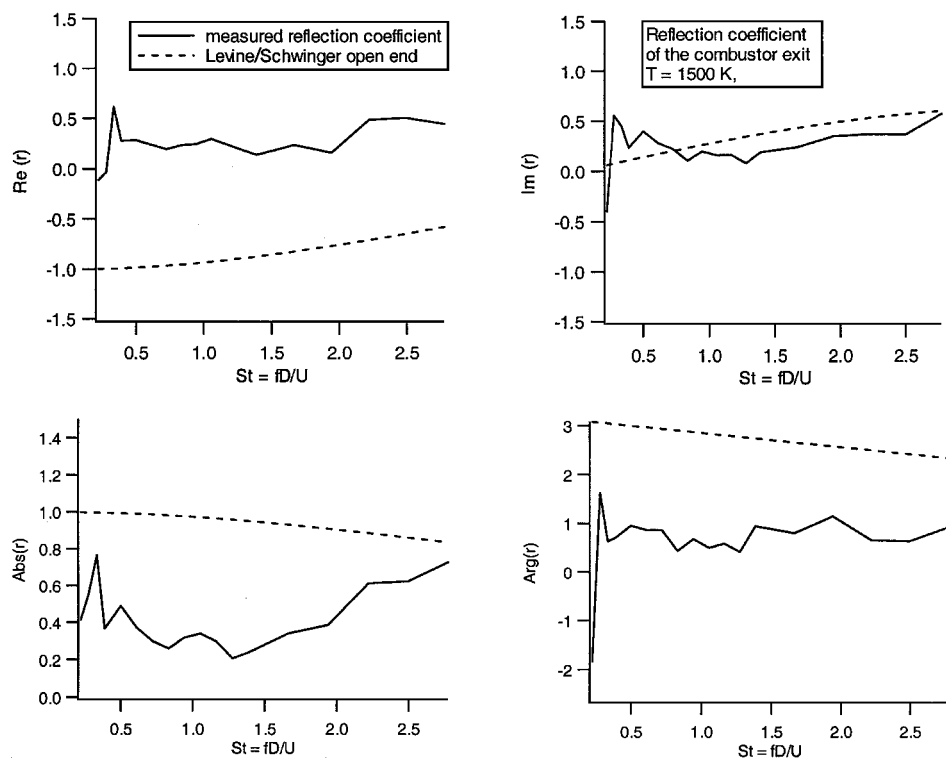


Fig. 2 Reflection coefficient of the low-reflecting acoustic boundary condition for the case with combustion. The dotted line displays the ideal open-end case following the theory of Levine and Schwinger.²¹

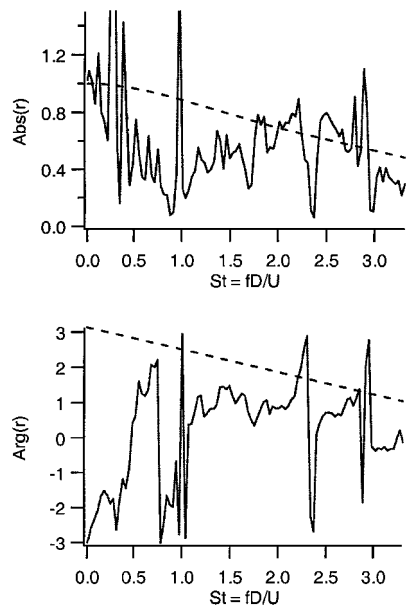


Fig. 3 Reflection coefficient of the low-reflecting acoustic boundary condition for the case without combustion. The dotted line displays the ideal open-end case following the theory of Levine and Schwinger.²¹

and radial cross spectra was significantly different (Figs. 5 and 6, respectively). It showed that upstream forcing was more effective in modifying the flow structure than the downstream forcing when applied to the axisymmetric mode ($St = 0.22$). Cross-spectra amplitudes corresponding to the upstream forcing were as much as six times higher than those of the downstream forcing. The response of the helical mode to both forcing methods was nearly identical. The coherence function of the axisymmetric mode along the combustor centerline stayed at a higher level than the coherence of the helical mode (Fig. 7). Upstream forcing preserved the high coherence level of the axisymmetric vortices over a longer range of axial distance compared with the downstream forcing. Once again, the difference

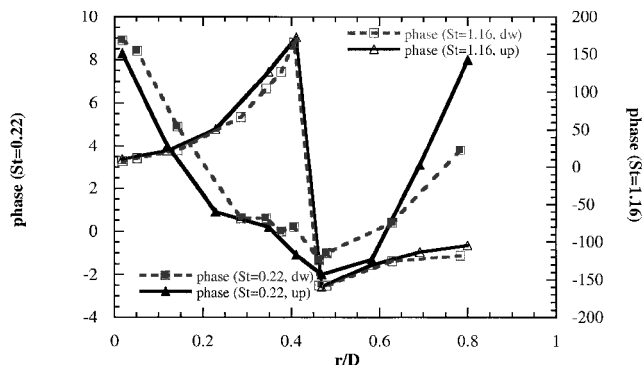


Fig. 4 Phase difference of the OH cross correlations at two forcing frequencies as a function of radial distance for a premixed-type flame. The effect of upstream and downstream forcing is compared.

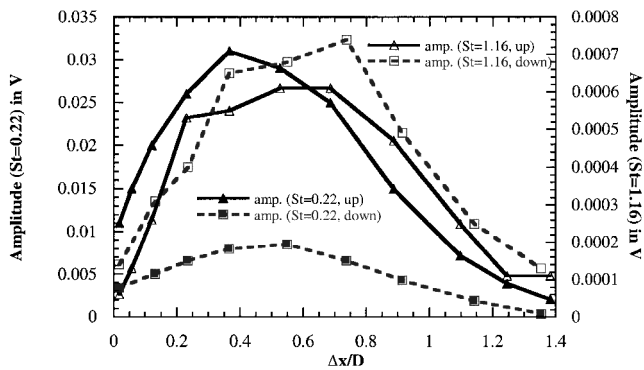


Fig. 5 Amplitude of the OH cross correlation at two forcing frequencies as a function of downstream distance measured in the shear layer for a premixed-type flame. The effect of upstream and downstream forcing is compared.

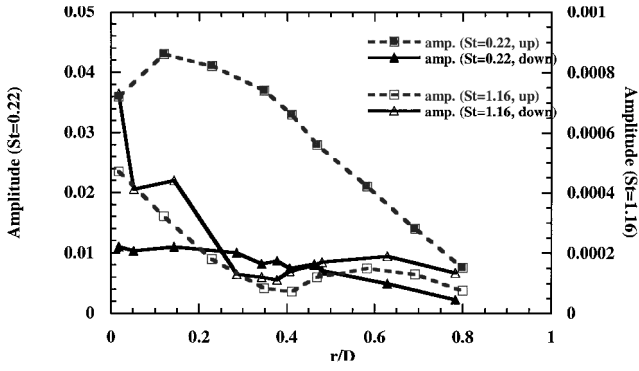


Fig. 6 Amplitude of the OH cross correlation at two forcing frequencies as a function of radial distance for a premixed-type flame. The effect of upstream and downstream forcing is compared.

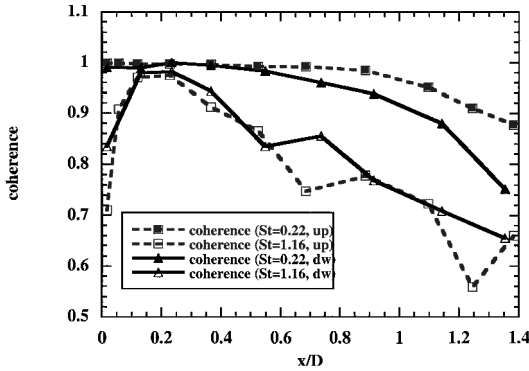


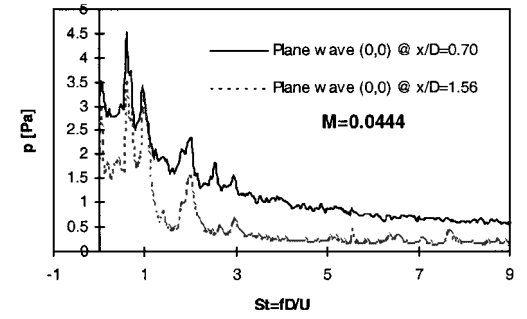
Fig. 7 Coherence of the OH cross correlations at two forcing frequencies as a function of downstream distance measured in the centerline for a premixed-type flame. The effect of upstream and downstream forcing is compared.

between the two forcing methods was not significant for the helical vortices. These tests suggest that upstream forcing is more effective in controlling the combustion instability than downstream forcing. It is conjectured that the upstream forcing could modify the evolution of the shear layer, whereas the downstream forcing relied on a combination of antisound principles and shear-layer excitation. The direct excitation of the shear-layer benefits from the natural amplification of the flow and thus requires less energy to obtain the same effect as noise cancellation. Similar observations were reported by Parr et al.⁹

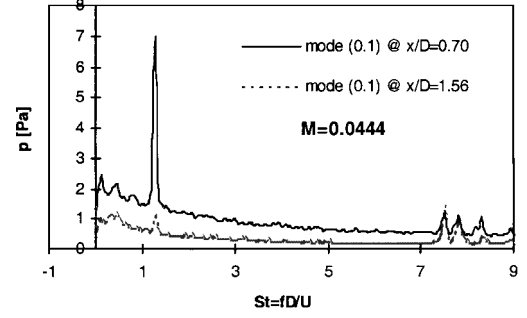
Thermoacoustic Instability Mode Structure

Flow Mode Structure

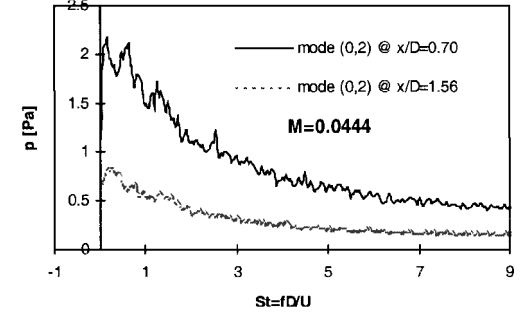
The mode structure of the flow was first investigated without combustion. The test rig used for this purpose had the same dimensions as the combustion test rig described in Fig. 1, and only a few changes were made to facilitate the measurements. The facility was instrumented with microphone and hot wires equally spaced around the circumference at 60 deg apart and at a number of axial locations up- and downstream of the burner nozzle. The first three modes are displayed in Fig. 8. Beside the plane wave mode ($m = 0$) at a normalized frequency $St = fD/\bar{U} = 0.6$, a strong helical mode ($m = 1$) at a normalized frequency $St = 1.2$ was observed. This mode was identified as a helical flow instability leading to pressure fluctuations, as observed using hot wires and in water-tunnel experiments.²² These tests showed the existence of a negative mean velocity region near the burner nozzle axis because of a recirculation region caused by vortex instability, which provides one of the mechanisms for flame stabilization in this burner nozzle. Consequently, the flow pattern near the axis was similar to wake flow behind a bluff body, which is mostly unstable to helical modes. The flow instability associated with this region was therefore predominantly helical, resembling wake flow instability. With increasing downstream distance the helical mode decreased by 16 dB over $x = 1D$. The plane wave mode was associated with the axisymmetric shear layer, which is formed



$m = 0$



$m = 1$



$m = 2$

Fig. 8 Mode structure without combustion at two downstream positions.

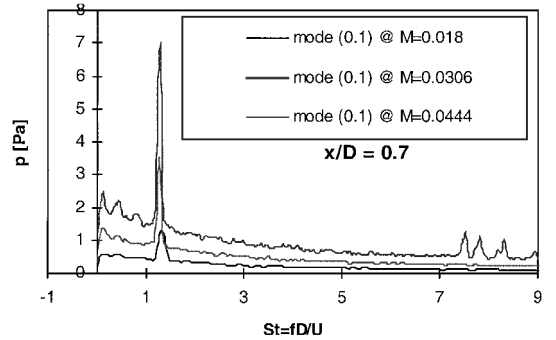


Fig. 9 First helical mode ($m = 1$) for different Mach numbers.

when the flow separates at the sudden expansion of the burner nozzle's exit.²² The flow did not exhibit a narrowband instability at mode $m = 2$. The first azimuthal acoustic resonant mode in the tube was at a Strouhal number $St = 7.8$ and was also captured in the $m = 1$ measurement. The source of this instability mode and its control were discussed in Paschereit et al.^{12,18} Below this frequency all higher modes were evanescent.

The helical $m = 1$ mode was scaled with the flow speed as shown in Fig. 9. The frequency increased proportionally with the flow speed and thus led to a constant normalized frequency $St = fD/\bar{U} = 1.2$.

Mode Structure with Combustion

The thermoacoustic instability modes were forced to occur by adjusting the acoustic boundary conditions for different combustor

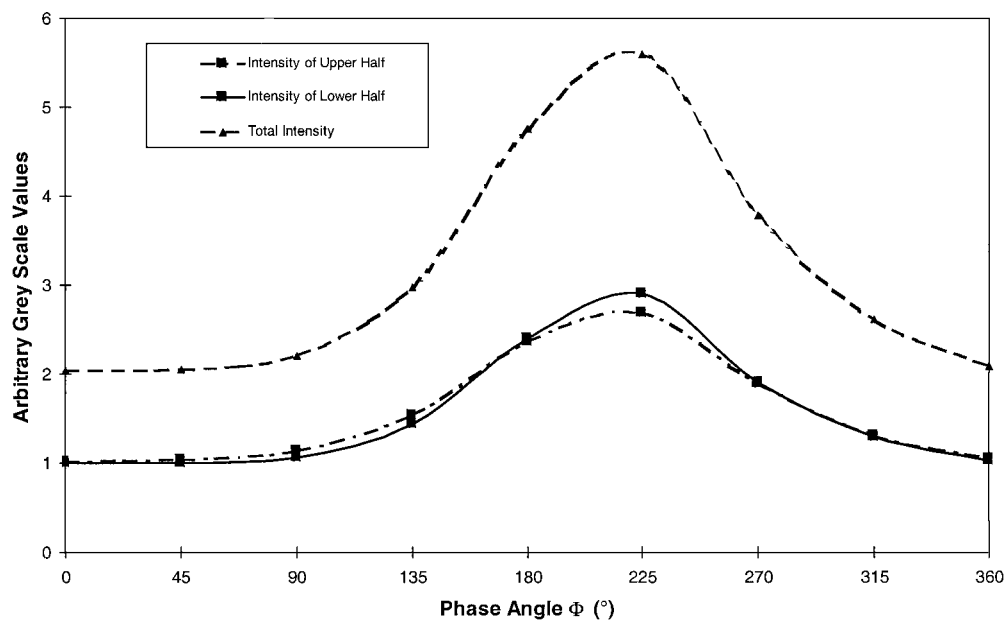


Fig. 10 Integrated OH radiation over the upper half and the lower half of the flame as well as over the entire flame of the low-frequency instability at $Sr = 0.58$ at various phase angles.

operating conditions. All of the instability modes were related to combustion within large-scale structures, which were excited in the combustion chamber caused by flow instabilities associated with the wake-like reversed shear flow near the axis and the separating flow at the sudden expansion. The flow instabilities were modified by the acoustic resonant modes of the combustor as determined by the combustion chamber acoustic boundary conditions.¹²

Some of the unstable frequencies measured by the pressure and OH signals were identical, but with different amplitudes. The instabilities associated with the premixed mode of operation occurred at a normalized frequency $Sr = f D / \bar{U} = 0.58$ (later characterized as an axisymmetric instability) and at $Sr = 1.16$ (which was determined to be a helical mode). The $Sr = 0.58$ instability was the predominant mode. A typical level of the $Sr = 0.58$ instability was 29 dB above the background noise level.

The different instability modes were visualized using an amplified and filtered CCD camera, which was triggered at different phase angles relative to the instability pressure signal. Using this technique, phase-averaged OH images were obtained for different thermoacoustic instabilities. An axisymmetric $Sr = 0.58$ instability mode was detected for a normalized equivalence ratio of $\phi / \phi_n = 1$ in a premixed combustion mode. Here, ϕ_n is the nominal equivalence ratio. The heat release at each phase angle was determined by integrating the OH emission over the upper half and the lower half of the flame as well as over the entire flame at each phase angle. These data are only qualitative in nature. The results are plotted during a full cycle in Fig. 10. The axisymmetric structure of this unstable mode is demonstrated as well as the cyclic variation of the heat release. The lowest heat release, which is related to the OH intensity, was measured at a zero phase angle, whereas the highest level was measured at 180 deg. The similar OH levels, which were obtained by integration over the upper and the lower half of the flame, characterize the axisymmetry of the flame structures.

In addition to the axisymmetric mode, a helical unstable mode was measured at the harmonic frequency ($Sr = 1.16$) with an equivalence ratio of $\phi / \phi_n = 1.1$ (Fig. 11). The measurements were done at the combustor premixed mode. The high OH intensity shifted from the upper shear layer for a phase angle of 90 deg to the bottom shear layer at 220 deg. A low-level planar acoustic forcing was applied to the burner nozzle and modified the helical flame structure, to an axisymmetric structure (Fig. 12). The integrated OH radiation over the upper half of the combustor and over its lower half, for the corresponding unforced helical flame and the forced axisymmetric flame, is shown in Figs. 13a and 13b, respectively. The upper half of the unforced flame shows maximum

heat release at a phase angle of 90 deg and a minimum at 270 deg. The lower half has a maximum at 220 deg and a minimum near zero. The phase differences between the two halves are characteristic of a quasi-helical structure. The axisymmetric structure of the forced flame is demonstrated by the nearly even and equal distributions of the integrated heat release in the two halves of the flame, as shown in Fig. 13b. The even distribution of heat release during the cycle indicates that the axisymmetric forcing suppressed the helical unstable mode, thus stabilizing the combustion.

Combustion Control

Pressure Oscillations

A closed-loop feedback control system was designed to reduce the coherence of the large-scale structures, thus to suppress the level of pressure oscillations caused by the axisymmetric mode of the combustion instability. This mode exhibited the strongest pressure oscillations. The sensor of the control system was a microphone, which picked up the acoustic resonance of the chamber and the control system and fed the signal back to the speakers. The phase between the microphone signal and the speakers' driving signal was varied between 0 and 360 deg. The effect on the pressure fluctuations amplitude at the instability frequency was recorded.

The control system was tested for two combustion modes: a premixed and a diffusion (partially premixed) mode. The diffusion flame corresponded to pilot flame operation. The variation of the pressure oscillations as a function of the relative phase between the microphone (sensor) and speakers (actuators) is shown in Fig. 14 for the axisymmetric unstable mode at $Sr = 0.58$ of the premixed combustion operation. The controlled behavior is compared with the straight horizontal line, which depicts the pressure fluctuations level when the controller is not operating. Maximum suppression was obtained at a phase difference of 270 deg, whereas maximum destabilization of the combustion was observed at 90 deg, 180 deg from the optimal angle. At the optimal phase angle the instability was suppressed by nearly 5 dB. The actual values of the optimal phase angles depend on the specific system design parameters such as the relative locations of the sensor, actuator, and flame.

A similar plot is shown in Fig. 14 for the diffusion flame. The instability frequency for this condition was at $Sr = 0.38$. Maximum suppression was about 3 dB at a phase angle of 230 deg. An increase of over 5 dB was observed at an angle of 40 deg. The absolute level of pressure oscillations, during instability, of the diffusion mode was lower than that of the premixed mode. Consequently, the suppression in the diffusion flame was not as effective as in the premixed case. Also, the diffusion flame was initiated further upstream than the

flow direction →

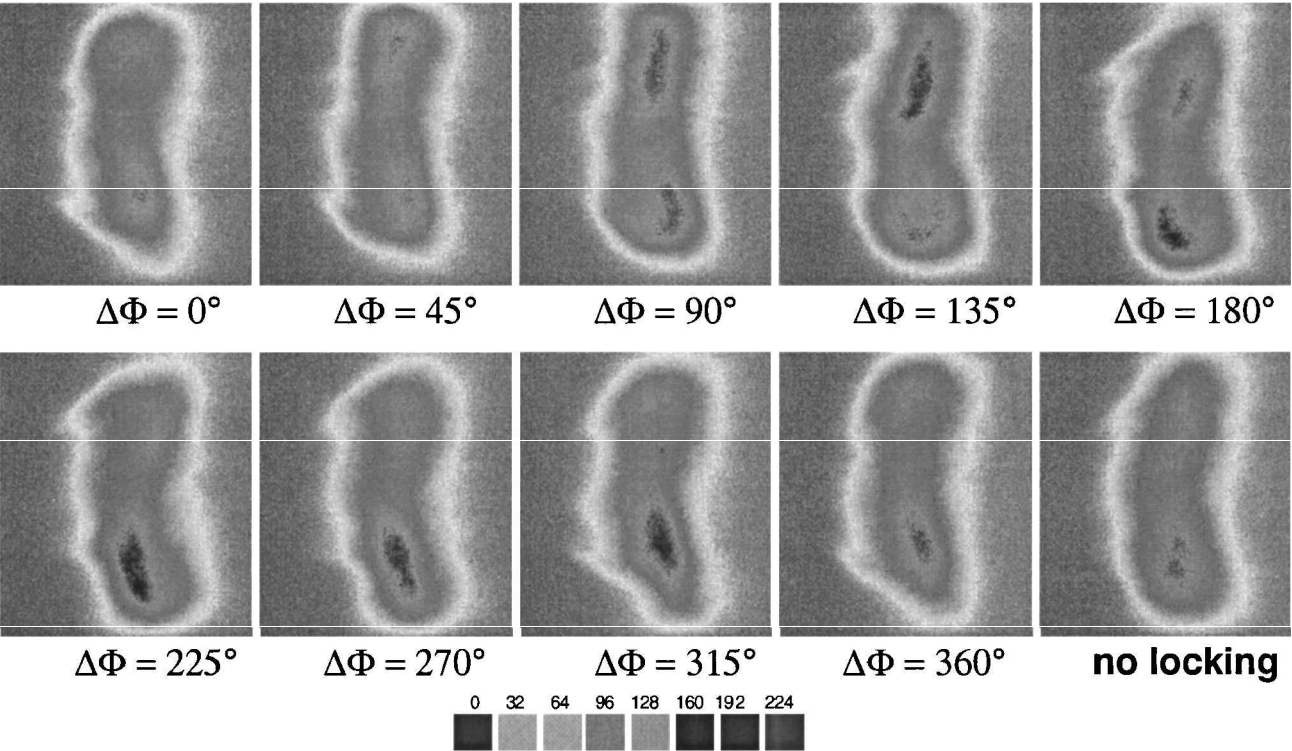


Fig. 11 Phase-averaged visualization of the helical instability at $Sr = 1.16$ at various phase angles. The images were filtered using a bandpass filter at $290\text{ nm} < \lambda < 390\text{ nm}$ and show the OH emission of the flame.

flow direction →

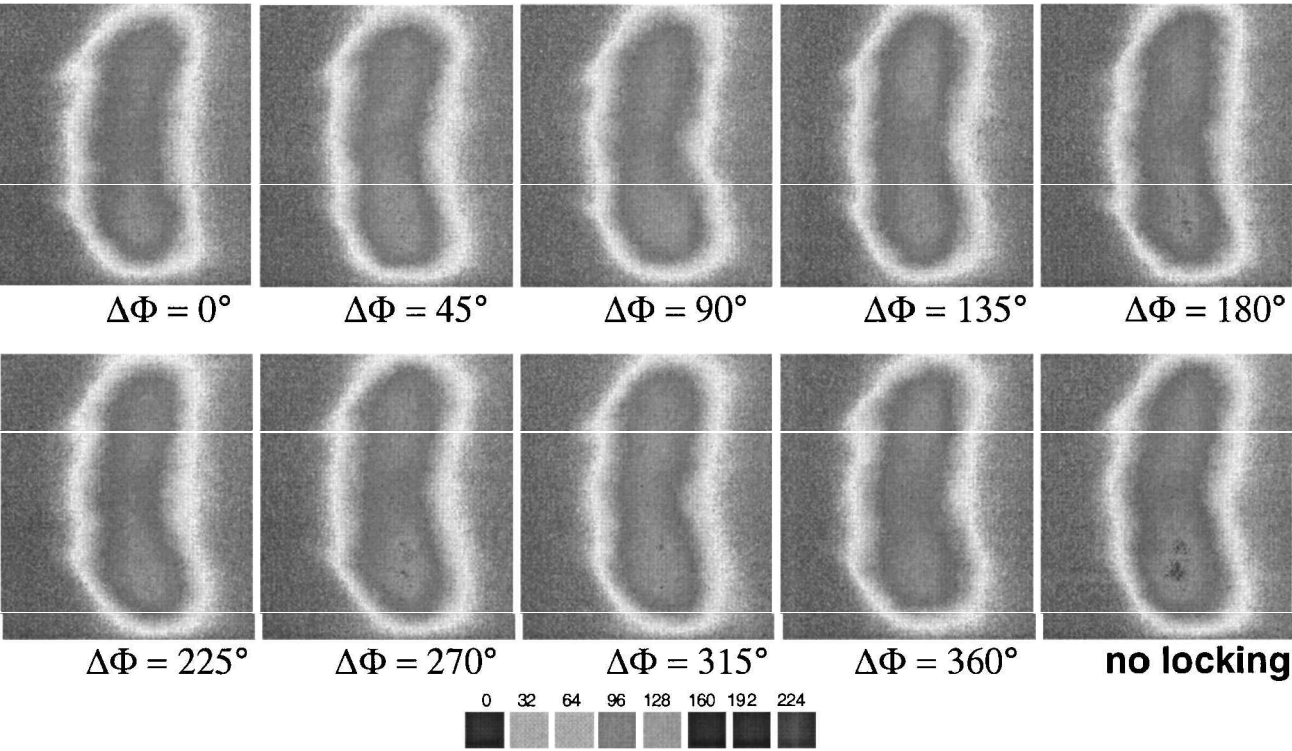


Fig. 12 Phase-averaged visualization of the helical instability at $Sr = 1.16$ at various phase angles. The images were filtered using a bandpass filter at $290\text{ nm} < \lambda < 390\text{ nm}$ and show the OH emission of the flame. In this case a low-amplitude axisymmetric forcing was applied, which destroys the helical structure.

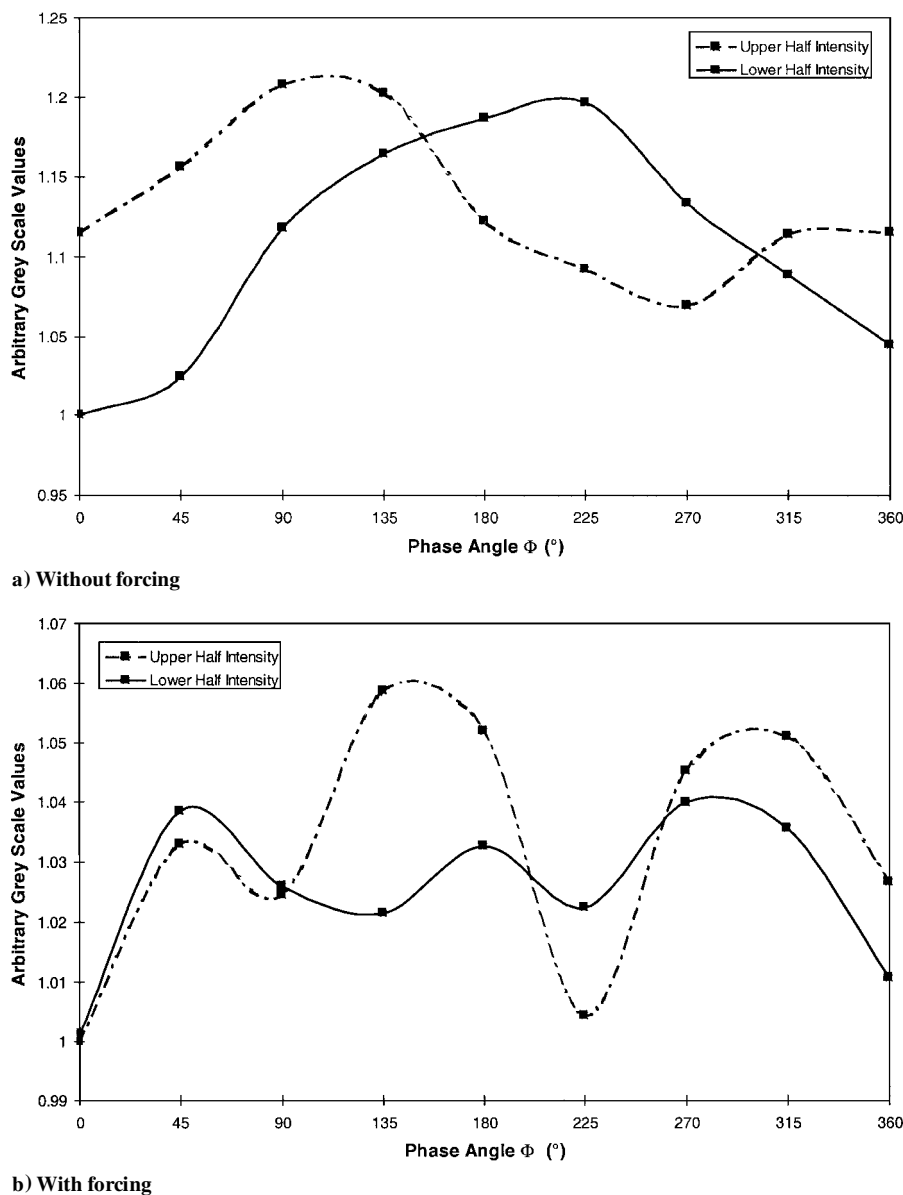


Fig. 13 Integrated OH radiation over the upper half and the lower half of the flame of the helical instability at $Sr = 1.16$ at various phase angles.

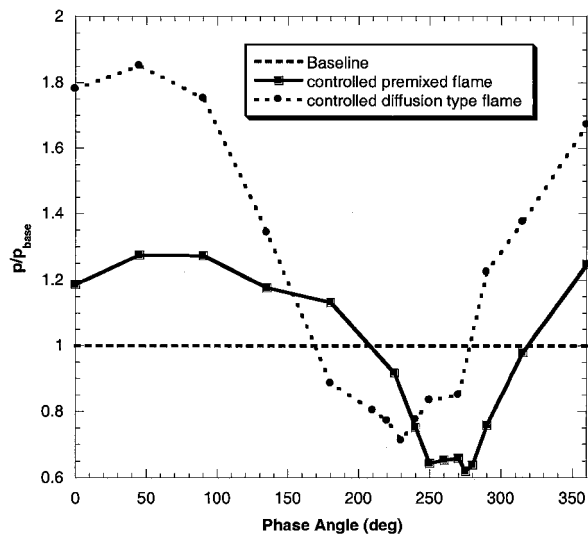


Fig. 14 Amplitude of the pressure oscillations at the instability frequency $Sr = 0.58$ (premixed combustion) and $Sr = 0.38$ (diffusion-type flame) for various phase shifts in a closed-loop control system with pressure locking.

premixed flame, well upstream of the shear-layer location, thus the interaction between the large-scale vortices and the combustion was reduced, causing the acoustic forcing to become less effective.

The amplitude of the control signal was varied to study its effect on the level of reduction of pressure oscillations at the optimal phase of 230 deg. The results shown in Fig. 15 indicate that a minimum of $F/F_{\max} = 40\%$ of the maximum forcing amplitude F_{\max} was necessary to reach the optimal control level.

Emissions of Pollutants

Emissions of NO_x were monitored at the entire range of phase angles for the microphone-based control system in both the premixed and diffusion combustion. The results of the premixed combustion, depicted in Fig. 16, show reduction of the NO_x levels at 270 deg phase difference relative to the baseline case. Increased emissions were observed at 90 deg. The reductions of both the NO_x emissions and the pressure oscillations occurred at the same phase angle and are related to the reduced coherence of the vortical structures when forcing was applied at this phase angle. Thermoacoustic instability can be associated with periodic combustion, which occurs when vortices are present. These vortices produce periodic high peak temperature, which leads to thermal NO_x formation. Control at a phase angle of 270 deg produces uniform mixing and improved combustion with evenly distributed temperature, yielding low NO_x

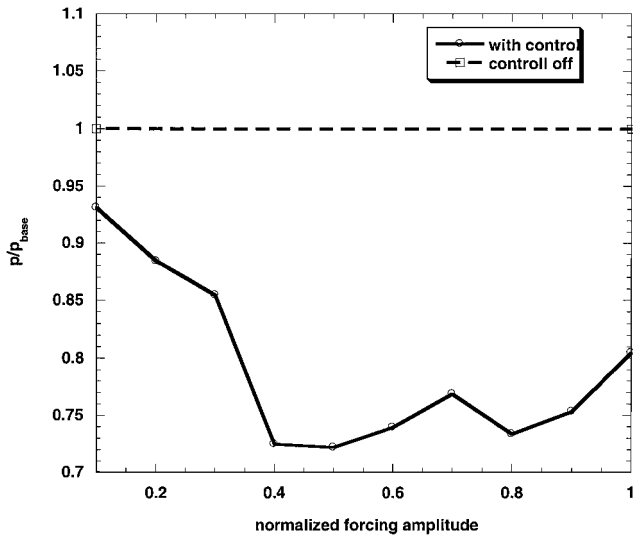


Fig. 15 Amplitude of the pressure oscillations at the instability frequency $Sr = 0.38$ for various forcing amplitudes in a closed-loop control system with pressure locking for a diffusion-type flame.

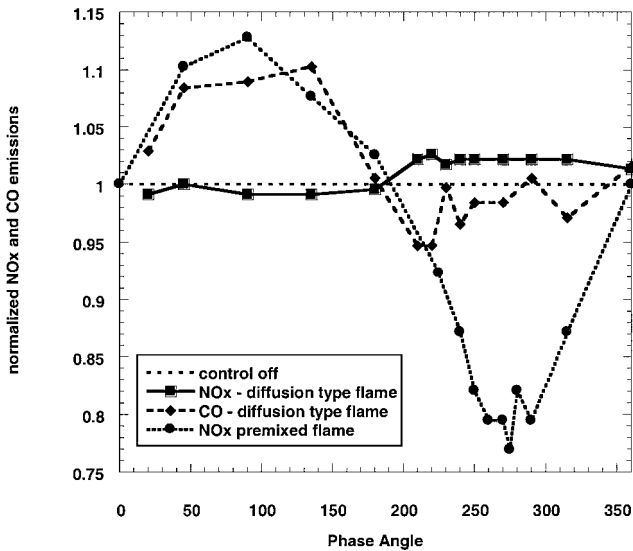


Fig. 16 Normalized NO_x and CO emissions for various phase shifts in a closed-loop control system with pressure locking for a premixed and a diffusion-type flame.

emissions. The decreased energy of coherent vortices with improved mixing inhibited the generation of peaks of heat release and locally high temperatures.

In the diffusion flame the results were quite different. The phase angle at which pressure oscillations were suppressed caused an increase in NO_x formation (Fig. 16). Some reduction was obtained at phase angles, which caused increased pressure oscillations. These observations suggest that the forcing at the phase angle that enhanced the thermoacoustic instability increased the local heat release and temperatures in the diffusion flame, possibly by enhanced mixing inside the burner nozzle, which was not necessarily associated with the large-scale vortices downstream of the burner nozzle exit. This suggestion is corroborated by the behavior of CO emissions during the control cycle (Fig. 16). The CO is somewhat reduced at the phase angles at which NO_x was increased and pressure fluctuations were reduced. An increase in CO formation was observed for the small phase angles. Low CO production is associated with high temperatures, which also generate high NO_x emissions.

Conclusions

Active combustion control was applied to an experimental low-emission swirl-stabilized combustor, in which the acoustic boundary

conditions were modified to obtain unstable operating conditions. Orifices with different exit areas were used to change the acoustic boundary conditions. The reflection coefficient was measured using a multimicrophone method that had better accuracy compared with the two-microphone method. An axisymmetric flame instability mode was obtained by adjusting the combustor length and the acoustic boundary condition at the combustor exit to an acoustic reflection coefficient $|r| > 0.5$, which yielded a longitudinal plane wave acoustic mode. When the acoustic boundary condition was adjusted to almost anechoic conditions $|r| < 0.2$, a helical flame instability was observed. However, the dominant unstable modes were axisymmetric.

The unstable modes were associated with flow instabilities related to the recirculation wake-like region on the combustor axis and shear-layer instabilities at the sudden expansion (dump plane), which could partly be verified in cold flow experiments. The combustion structure associated with the different unstable modes was visualized by phase-locked images of OH chemiluminescence. The axisymmetric mode showed large variation of the heat release during one cycle of oscillations, while the helical modes showed variations in the radial location of maximal heat release. Acoustic forcing was used to control the combustion instability and to modify its modal structure. Upstream acoustic excitation, which affected directly the evolution of the shear layer, was determined to be more effective than downstream excitation. The latter had a reduced effect on the shear-layer evolution and relied partially on noise cancellation. Forcing affected predominantly the axisymmetric mode. However, in some cases axisymmetric forcing transformed the helical mode into an axisymmetric one.

A closed-loop active control system was employed to suppress the thermoacoustic pressure oscillations and to reduce NO_x emissions by modifying the vortical structure of the combustor flow. Tests were performed for two combustion modes, i.e., premixed and diffusion flames. Microphone sensors were used to monitor the combustion process and provide input to the control system. A filtered signal of the microphone was phase shifted and amplified before being fed to the actuator. The upstream acoustic actuation was used to modulate the airflow before entering the swirl-generating burner nozzle. The acoustic excitation varied the mixing process between fuel and air and the combustion products and thus affected the combustion process. Suppression levels of up to 5 dB in the pressure oscillations and a concomitant reduction of NO_x emissions were obtained using an acoustic power of less than 0.002% of the combustor power in the premixed mode. The controller was less effective in the diffusion flame, leading to pressure reduction of less than 4 dB. With diffusion combustion the phase angles, which were effective in reducing the pressure oscillations, yielded an increase in NO_x and a decrease in CO emissions. The different effects of the control system on the premixed and diffusion flames were attributed to the difference in the location of the two flames relative to the burner nozzle exit plane. Although the premixed flame occurs in the shear layer downstream of the burner nozzle exit, the diffusion flame dynamics are partly decoupled from the shear-layer evolution because the flame was located further upstream.

At the optimal control conditions the major effect of the control system was shown to reduce the coherence of the vortical structures, which gave rise to the thermoacoustic instability. In the premixed combustion forcing decoupled the combustion process from the flow instability, the temperature became more uniform, and NO_x -forming high-temperature zones within vortices were eliminated while maintaining high combustion efficiency. In the diffusion flame the increased NO_x and reduced CO showed that the forcing-enhanced mixing inside the burner nozzle and increased local temperatures. Changes in equivalence ratio can be another driving mechanism for thermoacoustic instabilities. Based on pressure and velocity data,²² the equivalence ratio changes were estimated not to exceed 5% of the nominal value. However, OH changes during one cycle of oscillations corresponded to a change of nearly 50% variation of equivalence ratio relative to the baseline. This approximate estimation was based on a steady-state calibration of OH emissions at various equivalence ratios. Therefore the suggestion is made that this mechanism plays only a secondary role to the main mechanism related to flow instabilities.

Acknowledgments

We gratefully acknowledge the assistance of Jaan Völkening for the phase-averaged flame pictures and of Grant Anning for running the test rig and helping with the data analysis. The authors would also like to acknowledge the support of J. Hellat, J. J. Keller, ABB Power Generation Ltd., as well as K. Doebling and W. Polifke, ABB Corporate Research Ltd., to carry out this research.

References

- ¹Oster, D., and Wynanski, I., "The Forced Mixing Layer Between Parallel Streams," *Journal of Fluid Mechanics*, Vol. 123, 1982, pp. 91–130.
- ²Ho, C., and Huerre, P., "Perturbed Free Shear Layers," *Annual Review of Fluid Mechanics*, Vol. 16, 1984, pp. 365–424.
- ³Crow, S., and Champagne, F., "Orderly Structure in Jet Turbulence," *Journal of Fluid Mechanics*, Vol. 48, 1971, p. 567.
- ⁴Paschereit, C. O., Wynanski, I., and Fiedler, H. E., "Experimental Investigation of Subharmonic Resonance in an Axisymmetric Jet," *Journal of Fluid Mechanics*, Vol. 283, 1995, pp. 365–407.
- ⁵Hasan, M. A. Z., "The Flow over a Backward Facing Step Under Controlled Perturbation: Laminar Separation," *Journal of Fluid Mechanics*, Vol. 238, 1992, pp. 73–96.
- ⁶Schadow, K. C., and Gutmark, E., "Combustion Instability Related to Vortex Shedding in Dump Combustors and Their Passive Control," *Progress of Energy and Combustion Science*, Vol. 8, 1992, pp. 117–132.
- ⁷McManus, K. R., Poinso, T., and Candel, S. M., "A Review of Active Control of Combustion Instabilities," *Progress of Energy and Combustion Science*, Vol. 19, 1993, pp. 1–29.
- ⁸Annaswamy, A. M., and Ghoniem, A. F., "Active Control in Combustion Systems," *IEEE Control Systems*, Vol. 15, No. 6, 1995, pp. 49–63.
- ⁹Parr, T., Gutmark, E., Parr, D., and Schadow, K., "Feedback Control of an Unstable Ducted Flame," *Journal of Propulsion and Power*, Vol. 9, No. 4, 1993, pp. 529–535.
- ¹⁰Hsu, K. Y., Chen, L. D., Katta, V. R., Goss, L. P., and Roquemore, W. M., "Experimental and Numerical Investigations of the Vortex-Flame Interactions in a Driven Jet Diffusion Flame," AIAA Paper, Jan. 1993.
- ¹¹Gutmark, E., Parr, T. P., Wilson, K. J., Hanson-Parr, D. M., and Schadow, K. C., "Use of Chemiluminescence and Neural Networks in Active Combustion Control," *Twenty Third Symposium (International) on Combustion*, Combustion Inst., Pittsburgh, PA, 1990, pp. 1101–1106.
- ¹²Paschereit, C. O., Gutmark, E., and Weisenstein, W., "Structure and Control of Thermoacoustic Instabilities in a Gas-Turbine Combustor," *Combustion, Science and Technology*, Vol. 138, 1998, pp. 213–232.
- ¹³Paschereit, C. O., Gutmark, E., and Weisenstein, W., "Control of Thermoacoustic Instabilities and Emissions in an Industrial Type Gas-Turbine Combustor," *27th International Symposium on Combustion*, Combustion Inst., Pittsburgh, PA, 1998.
- ¹⁴Schadow, K. C., Gutmark, E., and Wilson, K. J., "Active Combustion Control in a Coaxial Dump Combustor," *Combustion, Science and Technology*, Vol. 81, 1992, pp. 285–300.
- ¹⁵Cohen, M. F., Rey, N. M., Jacobsen, C. A., and Anderson, T. J., "Active Control of Combustion Instability in a Liquid-Fueled Low-NO_x Combustor," American Society of Mechanical Engineers, 98-GT-267, June 1998.
- ¹⁶Seume, J. R., Vortmeyer, N., Krause, W., Hermann, J., Hantschk, C., Zangl, P., Gleis, S., Vortmeyer, D., and Orthmann, A., "Application of Active Combustion Instability Control to a Heavy Gas Turbine," *Journal of Engineering for Gas Turbines and Power*, Vol. 120, No. 4, 1998, pp. 721–726.
- ¹⁷Paschereit, C. O., and Polifke, W., "Investigation of the Thermoacoustic Characteristics of a Lean Premixed Gas Turbine Burner," American Society of Mechanical Engineers, Paper 98-GT-582, June 1998.
- ¹⁸Paschereit, C. O., Gutmark, E., and Weisenstein, W., "Control of Thermoacoustic Instabilities in a Premixed Combustor by Fuel Modulation," AIAA Paper 99-0711, Jan. 1999.
- ¹⁹Chung, J. Y., and Blaser, D. A., "Transfer Function Method of Measuring In-Duct Acoustic Properties. I, Theory," *Journal of the Acoustical Society of America*, Vol. 68, 1980, pp. 907–913.
- ²⁰Cattolica, R. J., "OH Radical Non-Equilibrium in Methane-Air Flat Flames," *Combustion, Science and Technology*, Vol. 44, 1982, p. 43.
- ²¹Levine, H., and Schwinger, J., "On the Radiation of Sound from an Unflanged Circular Pipe," *Physical Review*, Vol. 73, 1947, pp. 383–405.
- ²²Paschereit, C. O., Gutmark, E., and Weisenstein, W., "Coherent Structures in Swirling Flows and Their Role in Acoustic Combustion Control," *Physics of Fluids*, Vol. 11, No. 9, 1999, pp. 2667–2678.

J. P. Gore
Associate Editor